

## Supplementary Information for

### **Fabrication of novel g-C<sub>3</sub>N<sub>4</sub> based MoS<sub>2</sub> and Bi<sub>2</sub>O<sub>3</sub> nanorods embedded ternary nanocomposites for superior photocatalytic performance and destruction of bacteria**

***Shanmugam Vignesh*<sup>1</sup>, *Jeyaperumal Kalyana Sundar*<sup>1\*</sup>, *Mariappan Pandiaraman*<sup>2</sup>, *Anna Lakshmi Muppudathi*<sup>3</sup>**

*<sup>1</sup> Materials Science Research Laboratory, Department of Physics, Periyar University, Salem - 636 011, Tamil Nadu, India*

*<sup>2</sup> PG and Research Department of Physics, Raja Doraisingam Govt. Arts College, Sivagangai - 630 561, Tamil Nadu, India*

*<sup>3</sup> Department of Physics, ERK Arts and Science College, Dharmapuri - 636 905, Tamil Nadu, India*

#### **\*Corresponding Author**

Dr. J. Kalyana Sundar (Email: jksundar50@gmail.com)

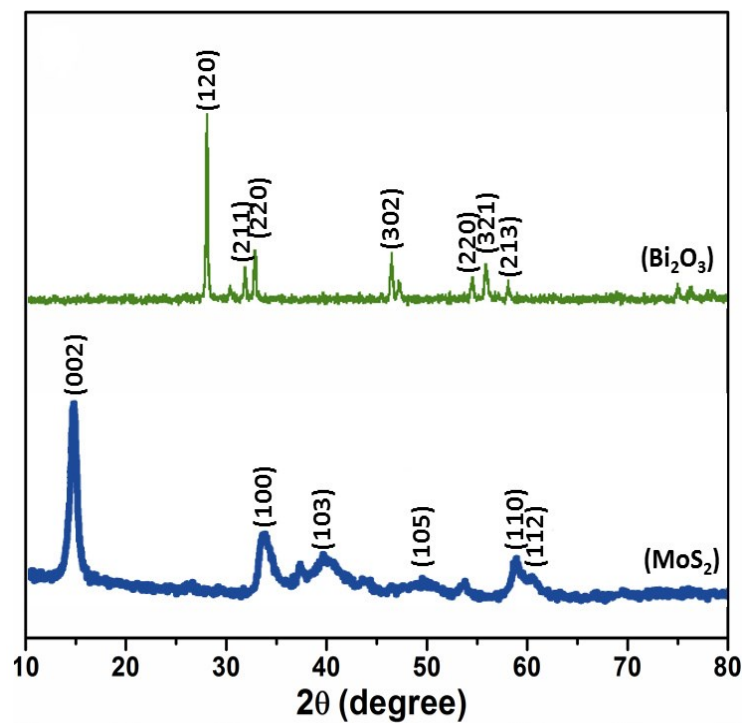


**Fig. S1** XRD pattern of as-obtained pristine  $\text{MoS}_2$  and  $\text{Bi}_2\text{O}_3$  nanomaterials

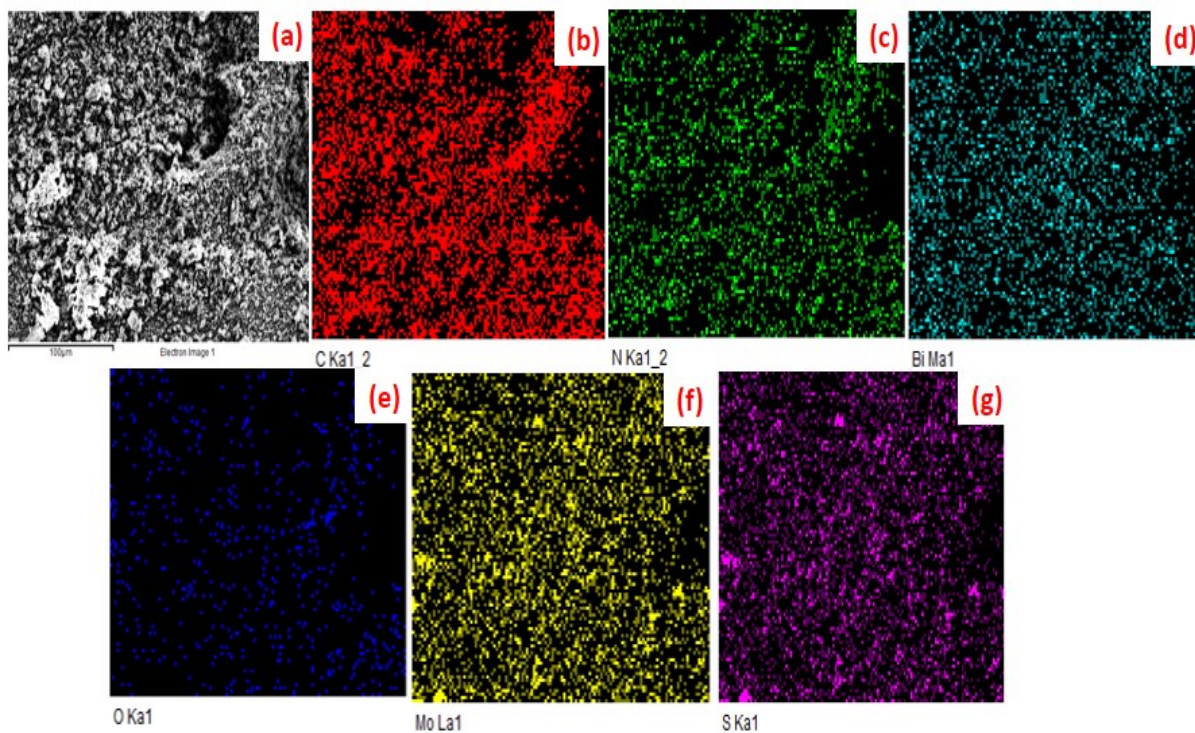


**Fig. S2** Elemental mapping analysis of  $\text{g-C}_3\text{N}_4/\text{MoS}_2/\text{Bi}_2\text{O}_3$  nanocomposite

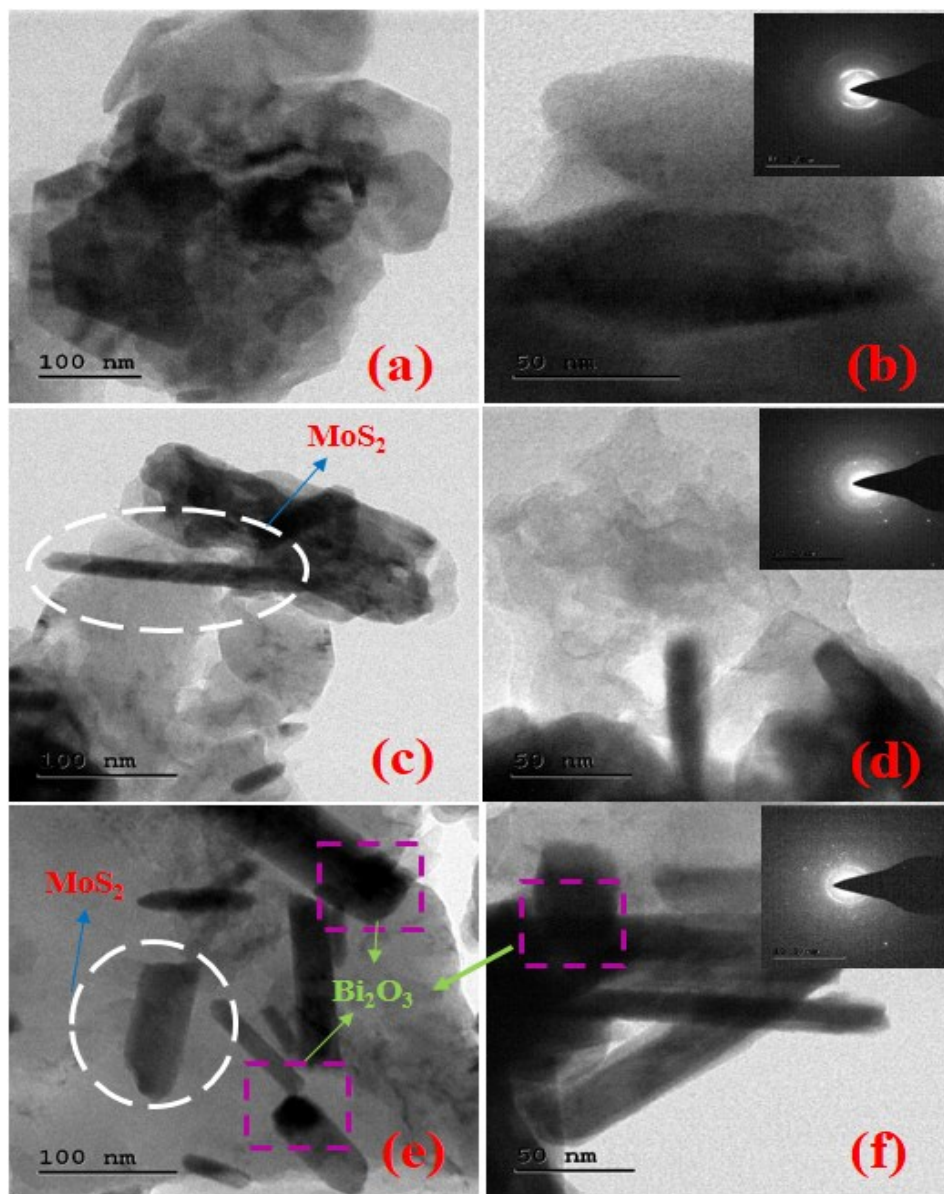


**Fig. S3** HR-TEM images of (a, b)  $g\text{-C}_3\text{N}_4$  (c, d)  $g\text{-C}_3\text{N}_4/\text{MoS}_2$  and (e, f)  $g\text{-C}_3\text{N}_4/\text{MoS}_2/\text{Bi}_2\text{O}_3$  nanorods embedded nanocomposites and corresponding SAED pattern

### S1. Depiction of Electrochemical investigation

The electrochemical execution of as-arranged samples was tried on a CHI-760 electrochemical workspace in an ordinary three-electrode conspire comprising of Ag/AgCl (in soaked KCl) as a kind of reference electrode, Pt wire by a counter electrode, and test covered Indium doped Tin oxides (ITO) glass for working electrode.  $\text{Na}_2\text{SO}_4$  (0.5 M; 50 ml of D.I water) fluid arrangement <sup>1</sup> was used by the electrolyte. The working electrode was composed as

pursues: 25 mg of the granulated sample was coupled by 20 mL of ethanol absolute in a testing tube, trailed by amassing of acetone to involved and ultra-sonication the slurry for 2 h. In addition, the clear dispersion was moved to 20 mL glass beaker and two bits of (2 cm × 0.5 cm) ITO glass was destroyed in the dissemination inside +10V to -10V for 10 minutes. Light irradiation was used in the photocurrent examinations was from a Xe lamp with several incidences with a time of light in ON and OFF settings. In addition, the main functionalization of EIS bends were gotten at - 0.4 V versus Ag/AgCl.

## S2. Photocatalytic Phenol degradation

Phenol is a noxious and carcinogenic complex usually originate in industrial wastewater. It causes severe threats to the ecology and to humanoid health. In this current study, g-C<sub>3</sub>N<sub>4</sub>/MoS<sub>2</sub>/Bi<sub>2</sub>O<sub>3</sub> nanocomposite has been used and are active in the photocatalytic deprivation of phenol. Still, to the best of our data, revisions on the g-C<sub>3</sub>N<sub>4</sub>/MoS<sub>2</sub>/Bi<sub>2</sub>O<sub>3</sub> photocatalytic system are infrequent, and no reading has been stated on the photodegradation of phenol by g-C<sub>3</sub>N<sub>4</sub>/MoS<sub>2</sub>/Bi<sub>2</sub>O<sub>3</sub> NCs. The photocatalytic concerts of the g-C<sub>3</sub>N<sub>4</sub>/MoS<sub>2</sub>/Bi<sub>2</sub>O<sub>3</sub> PCs were assessed by decaying phenol under visible-light revelation <sup>2</sup>.

### S2.1 Photocatalytic Analysis

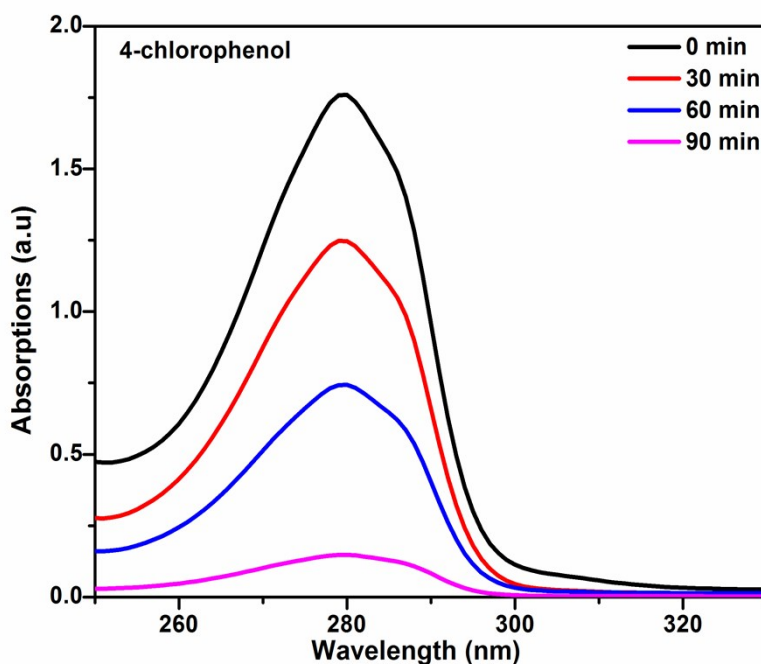


**Fig. S4.** UV-Vis absorption spectra of phenol over the g-C<sub>3</sub>N<sub>4</sub>/MoS<sub>2</sub>/Bi<sub>2</sub>O<sub>3</sub> composite under visible-light exposure

The photocatalytic enactment was appraised by the degradation of 4-chlorophenol, and experiments were carried out using a photocatalytic reactor with visible light were provided by a (500 W) halogen lamp by identical conditions. A mixture of 50 mg of the  $g\text{-C}_3\text{N}_4/\text{MoS}_2/\text{Bi}_2\text{O}_3$  PCs and 10 mL of phenol ( $10 \text{ mg L}^{-1}$ ) was mixed into 100 mL of D.I water and it used for photocatalysis process <sup>3</sup>. The UV-Vis absorption spectrum was exploited to explore the deviations of 4-chlorophenol and its photo-degradation intermediates besides with the exposure time. Figure S4 displays a decrease in the 4-chlorophenol absorbance at  $\lambda = \sim 279 \text{ nm}$  in the presence of  $g\text{-C}_3\text{N}_4/\text{MoS}_2/\text{Bi}_2\text{O}_3$  PCs under visible-light, lastly, 4-chlorophenol could be absolutely (92 %) degraded after 90 min of photo-reaction. This designated that 4-chlorophenol was oxidized to a complex mixture of visible-light and intermediates of catalysts, whereas the deficiency of absorption spectra might propose that the  $g\text{-C}_3\text{N}_4/\text{MoS}_2/\text{Bi}_2\text{O}_3$  PCs has a promising catalyst for different organic pollutant degradation of environmental remediation.

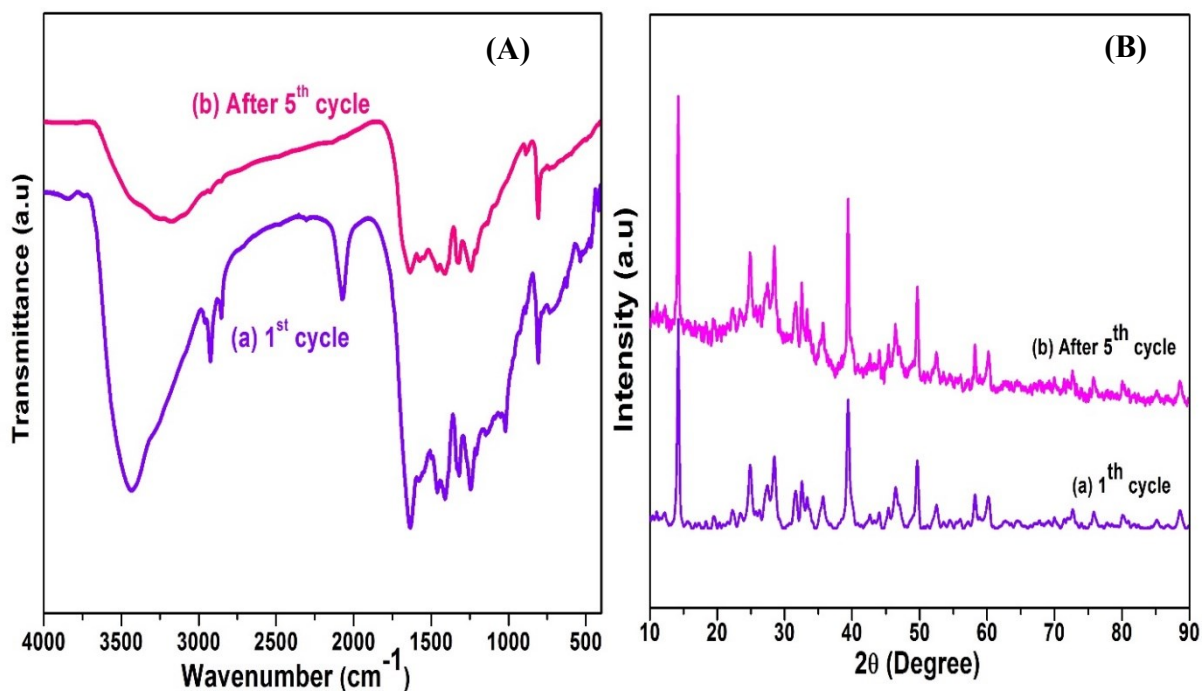


**Fig. S5.** (A) XRD and (B) FT-IR results of before and after MB dye photodegradation processed  $g\text{-C}_3\text{N}_4/\text{MoS}_2/\text{Bi}_2\text{O}_3$  samples

By the way of probable mechanism, the  $g\text{-C}_3\text{N}_4/\text{MoS}_2/\text{Bi}_2\text{O}_3$  PCs suspension under visible-light exposure, the enhanced photocatalytic system might be fashioned amid  $\text{MoS}_2/\text{Bi}_2\text{O}_3$  and  $g\text{-C}_3\text{N}_4$ .

C<sub>3</sub>N<sub>4</sub>, through which electrons (e<sup>-</sup>) on the CB of MoS<sub>2</sub> and/or Bi<sub>2</sub>O<sub>3</sub> migrate to the VB of g-C<sub>3</sub>N<sub>4</sub> and syndicate by h<sup>+</sup> within. Such migration of (e<sup>-</sup>) might extend the lifetime of (e<sup>-</sup>) on the CB of g-C<sub>3</sub>N<sub>4</sub> and h<sup>+</sup> on the VB of MoS<sub>2</sub>/Bi<sub>2</sub>O<sub>3</sub>. Based on the above analyses, the charge migration across the photocatalytic organization which facilitates the capable charge separation, and hence conserving the further species for oxidation and reduction of organic pollutants of MB and colourless phenol as well.

### S3. The description of Analysis of Antibacterial Activity

The assessment of antibacterial inhibition zone of the readied nanocomposites was additionally tried by the well-diffusion technique. In this investigation, (G<sup>+</sup>) *S. aureus* and (G<sup>-</sup>) *E. coli* microscopic organisms were utilized for the run of the mill living being, which by characterizing the antibacterial properties of the readied tests by means of zone inhibition technique <sup>4</sup>. An appropriate proportion of the readied tests was then delicately situated on the LB agar plates. In such the fixation arrangement was 50, 100, 150 and 200 µg/ml and the dishes were brooded circumstance for 24 h on 37 °C. Subsequently, the activity was resolved by figuring the (ZOI) zone of the inhibition-free zone with no bacterial development that had conformed to each example, and the results were recorded and organized by Table S1.

**Table. S1** Antibacterial activity of as-obtained nanocomposites against different microorganisms

Samples	Inhibition zone (mm)							
	<i>E. coli</i>				<i>S. aureus</i>			
	50 µg	100 µg	150 µg	200 µg	50 µg	100 µg	150 µg	200 µg
g-C <sub>3</sub> N <sub>4</sub>	7±0.0	7±0.5	8±0.5	8±0.5	6±0.5	7±0.5	7±1	7±0.5
g-C <sub>3</sub> N <sub>4</sub> /MoS <sub>2</sub>	8±0.5	9±0.5	9±0.5	11±1	7±0.5	9±1	10±0.0	10±0.5
g-C <sub>3</sub> N <sub>4</sub> /MoS <sub>2</sub> /Bi <sub>2</sub> O <sub>3</sub>	10±0.5	11±1	11±0	11±0.5	12±0.5	13±0.5	12±1.0	13±0.5



## References

- 1 S. Liu, J. Chen, D. Xu, X. Zhang and M. Shen, *Journal of Materials Research*, 2018, **33**, 1391–1400.
- 2 Z. Wei, F. Liang, Y. Liu, W. Luo, J. Wang, W. Yao and Y. Zhu, *Applied Catalysis B: Environmental*, 2017, **201**, 600–606.
- 3 H.-T. Ren, S.-Y. Jia, Y. Wu, S.-H. Wu, T.-H. Zhang and X. Han, *Industrial & Engineering Chemistry Research*, 2014, **53**, 17645–17653.
- 4 W. Yin, J. Yu, F. Lv, L. Yan, L. R. Zheng, Z. Gu and Y. Zhao, *ACS Nano*, 2016, **10**, 11000–11011.